

Resilient UAV Formation for Coverage and Connectivity of Spatially Dispersed Users

Yuhui Wang and Junaid Farooq

Department of Electrical and Computer Engineering,
University of Michigan-Dearborn, Dearborn, MI 48128 USA.

Emails: {ywangdq, mjfarooq}@umich.edu

Abstract—Unmanned aerial vehicles (UAVs) are a convenient choice for carrying mobile base stations to rapidly setup communication services for ground users. Unlike terrestrial networks, UAVs do not have fiber optic back-haul connectivity except when they are tethered to the ground, which restricts their mobility. In the absence of back-haul, e.g., in remote areas, emergency situations, or in battlefields, there is a need to ensure connectivity among UAVs in addition to coverage of ground users for creating local area networks. This paper provides a distributed and dynamic approach for UAV formation-based control for coverage and connectivity of spatially dispersed users. We use flocking dynamics as a guide to constructing tailored formations of UAVs on the fly. Simulation results demonstrate that if sufficient aerial base stations are available, the proposed approach results in a strongly connected network of UAVs that is able to provide both a backhaul and fronthaul network. The approach can be further extended to create multi-tier extra-terrestrial networks to cater for large-scale applications.

Index Terms—unmanned aerial vehicles, connectivity, resilience, distributed algorithm.

I. INTRODUCTION

Unmanned aerial vehicles (UAVs) are now becoming widespread in a range of smart city applications such as package delivery, policing, transportation, etc. UAVs are also considered to play a key role in the next-generation of wireless networks (i.e., 6G and beyond) [1][2], where it can support and enhance existing cellular infrastructure to connect the unconnected. UAVs carrying base stations (BSs) can be crucial in providing communication services in certain situations such as in disaster-struck areas and battlefields [3]. In fact, tethered drones are already providing connectivity in emergency situations, e.g., AT&T cell on wings (COWs) were used in recent hurricane Ida in Louisiana to restore LTE coverage to cellular users [4]. However, these operations are on a limited scale and typically supplement existing cellular networks by relying on already available back-haul links [5].

To scale up the deployment of aerial platforms for creating local area networks, there is a need to develop adaptive strategies that are able to maintain UAV connectivity while ensuring the ground users are reachable.

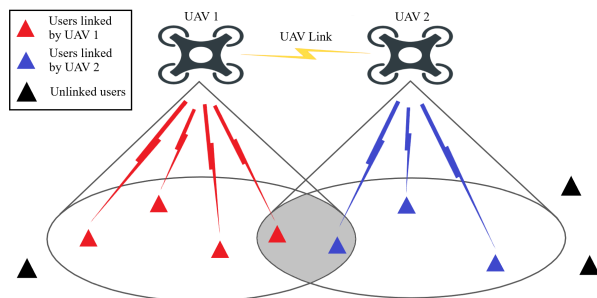


Fig. 1: Illustration of coverage and connectivity for two UAVs. The UAVs remain in close proximity of each other and also connect to ground users within their coverage range.

Fig. 1 illustrates a simple scenario where two UAVs are connected to ground users within their communication range while being in close proximity to each other. This enables the formation of a local network in the absence of a back-haul. However, an extended relay network of UAVs can also connect to the wider back-haul networks via tethered links, satellite communication, or other terrestrial networks. The key challenge is to design and dynamically achieve a UAV network formation that is tailored to the locations of ground users.

The problem of creating a formation that covers users and also ensures close proximity of the UAVs is an NP-hard problem, particularly in cases when the underlying users are located in geographically dispersed clusters. In many ways, it is similar to the facility location problem in Operations Research and supply chain management [6], where facility centers need to be positioned at locations that best serves the demands of consumers. However, the additional constraint here is to ensure that facilities are close enough to create a lattice structure, which makes the problem intractable.

We use a completely distributed and dynamic approach to tackle this problem inspired from swarming or flocking dynamics in robotics and control literature. UAVs achieve the desired formations by operating in multiple modes including goal navigation, network con-

nectivity establishment and user coverage optimization, which provide a natural and holistic approach to solve such multi-layer problems.

II. RELATED WORK

Existing works in the literature on UAV placement use static optimization algorithms for selecting optimal UAV locations based on various goals and objectives, e.g., maximal coverage [7], minimizing coverage holes [8], [9]. Most works assume the availability of back-haul networks or use ground communication infrastructure as a supplement to UAV networks. Traditional operations research based approaches such as disk covering and bin packing have also been investigated for UAV drones [10]. However, they are unable to ensure connectivity among them. We have considered a completely standalone UAV system for both coverage and connectivity purposes.

A preliminary version of the framework has been presented in [11][12] where a flocking based control algorithm creates a formation that can provide both coverage to the users while keeping the UAVs connected [13]. However, it is only limited to scenarios where the ground users are in close proximity to each other. In other words, it does not support more complex user distributions especially where the users are spatially dispersed. In this work, we have enhanced the framework with a multi-modal system that can ensure that UAVs can participate in coverage of clusters as well as in connecting different clusters in a distributed fashion. Furthermore, the proposed dynamic approach is naturally able to adapt to changes that occur in the network over time as opposed to static optimization approaches that are not resilient to failures and attacks.

III. SYSTEM MODEL

Consider a set of ground users referred to as mobile smart devices (MSDs) $\mathcal{M} = \{1, \dots, M\}$, that are placed arbitrarily in \mathbb{R}^2 and a set of UAVs, referred to as mobile access points (MAPs) $\mathcal{L} = \{1, \dots, L\}$, that are each placed at a height of $H_i \in \mathbb{R}^+$, $i = \{1, \dots, L\}$. The Cartesian coordinates of the MSDs at time t are denoted by $\mathbf{y}(t) = [y_1(t), y_2(t), \dots, y_M(t)]^T$, where $y_i(t) \in \mathbb{R}^3, \forall i \in \mathcal{M}, t \geq 0$. Similarly, the Cartesian coordinates of the MAPs at time t are denoted by $\mathbf{q}(t) = [q_1(t), q_2(t), \dots, q_L(t)]^T$, where $q_i(t) \in \mathbb{R}^3, \forall i \in \mathcal{L}, t \geq 0$. The velocity of the MAPs at time t are denoted by $\mathbf{p}(t) = [p_1(t), p_2(t), \dots, p_L(t)]^T$, where $p_i(t) \in \mathbb{R}^3, \forall i \in \mathcal{L}, t \geq 0$. We assume that the MSDs are partitioned into $K \in \mathbb{Z}^+$ geographically separated sets $\mathcal{S} = \{S_1, S_2, \dots, S_K\}$ and the centroid of each set or cluster S_i is denoted by C_i .

The MAPs have a maximum communication range of $r \in \mathbb{R}^+$ such that any two MAPs can communicate

only if the Euclidean distance between them is less than r . The communication neighbours of each MAP is represented by the set $N_i = \{j \in \mathcal{L}, j \neq i : \|q_i - q_j\| \leq r\}, \forall i \in \mathcal{L}$. The quality or strength of the communication links between the MAPs is modeled using a distance dependent decaying function $\alpha_{z_1, z_0}(z) \in [0, 1]$ with finite cut-offs, expressed as follows [14]:

$$\alpha_{\{z_1, z_0\}}(z) = \begin{cases} 1, & \text{if } 0 \leq z < z_1, \\ \frac{1}{2} \left(1 + \cos\left(\pi \frac{z-z_1}{z_0-z_1}\right) \right), & \text{if } z_1 \leq z < z_0, \\ 0, & \text{if } z \geq z_0, \end{cases} \quad (1)$$

where z_0 and z_1 are constant cut-offs.

As the MSD to MAP path-loss [15] is distance dependent, we assume an MSD i always establishes connection with the MAP offering best quality of service:

$$j = \arg \max_{k \in \mathcal{L}: \|y_i - q_k\| \leq r} \rho \|y_i - q_k\|^{-\eta}, \quad (2)$$

where $\rho \in \mathbb{R}^+$ is the transmission power and $\eta \in \mathbb{R}^+$ is the pass-loss exponent. The number of MSDs connected to each MAP is denoted by N_u^k , $k \in \mathcal{L}$.

A. MAP Dynamics

We leverage the widely accepted kinematic model in robotics and control literature to describe the dynamics of the MAPs as follows:

$$\begin{aligned} \dot{q}_i &= p_i, \\ \dot{p}_i &= u_i, \end{aligned} \quad (3)$$

where $q_i, p_i, u_i \in \mathbb{R}^3$ and $i \in \mathcal{L}$. The control input can be designed to consist of the following three terms:

$$u_i = f_i + g_i + h_i, \quad (4)$$

where f_i is an inter-MAP attractive/repulsive term, g_i is a velocity consensus term, h_i is a term defining the individual target of each MAP.

B. Coverage and Connectivity

The network coverage can be determined by the proportion of MSDs in the network that are successfully connected to an MAP. It is referred to as the coverage ratio of the network, R_c and can be determined as follows:

$$R_c = \frac{1}{M} \sum_{i=1}^L N_u^i, \quad (5)$$

It reflects the formation status of MAPs and is used as a criteria in the mode switching.

The connectivity of the MAP network can be measured in terms of its Fiedler value (i.e., the second-smallest eigenvalue of the Laplacian matrix L) [16]. The adjacency matrix $\mathbf{A} = [a_{i,j}]$ is defined as:

$$a_{i,j} = \begin{cases} 1, & \text{if } \|q_i - q_j\| \leq r, \\ 0, & \text{otherwise,} \end{cases} \quad (6)$$

where $i, j \in \mathcal{L}$. The Laplacian matrix of the MAP network is defined as $L = D - A$ with D as the degree matrix of A . The Fiedler value is non-zero if each MAP in the network is reachable from any of the other MAPs, and hence provides a useful measure of global network connectivity. Furthermore, the higher the Fiedler value, the more robust and resilient the network will be from a connectivity standpoint.

IV. METHODOLOGY

This section presents the methodology used to develop the coverage formation and the connectivity establishment for MAPs. We create a resilient and autonomous configuration of MAP network through a multi-modal coverage control algorithm.

A. Multi-modal Coverage Control

In order to create tailored formations of MAPs to cover the MSDs in the network, we need to create several different modes of operation for the MAPs. Assume the centroids $\mathcal{C} = \{C_1, C_2, \dots, C_k\}$ of all MSD clusters $\mathcal{S} = \{S_1, S_2, \dots, S_k\}$ are known and the MAPs keep a minimum-weight spanning tree (MST) of MSD clusters that are already covered $\mathcal{T}_c = \{S_c^1, S_c^2, \dots, S_c^k\}$. At any given time, each MAP can be in one of the following operation modes:

- M_0 : When in Dynamic mode, the MAP sets its goal to the nearest cluster center C_i that is not covered and travels to the cluster.
- M_1 : When in Connectivity mode, the MAP determines the next cluster to connect and establish connectivity based on distributed MST algorithm [17].
- M_2 : When in Static mode, the MAP stays and serves MSDs in its goal cluster.

The initial modes of all MAPs are set to $M_i(0) = M_0$. In each iteration, each MSDs match with the nearest MAP using (2), and the MAPs share information such as relative position, velocity, number of connected MSDs, etc. with their neighbors. Then the network-wide coverage ratio is used for the switching modes and computing dynamics. The control algorithm is shown in Algorithm 1.

B. Connectivity Potential

In order to form connectivity between clusters, we design a connectivity potential based on positions of cluster centroids. Suppose the MAP i connects clusters S_1 and S_2 with centroids C_1 and C_2 respectively. In practice, the cluster centers can be determined by an aerial survey of the ground population and users. Several techniques such as simultaneous localization and mapping (SLAM) and other imaging technologies are now available that can automate the process to provide

Algorithm 1 MAP Control

Require: Initialize position, velocity and mode for each MAP $q_i(0), p_i(0), M_i(0) \leftarrow M_0$.

- 1: **while** not converged **do**
 - 2: Determine the number of connected MSDs for each MAPs ($N_u^i(k)$).
 - 3: Each MAPs share the position, velocity, number of connected MSDs, list of achieved goals with its neighbors.
 - 4: Determine network-wide coverage ratio.
 - 5: Each MAP updates mode $M(k)$ using Algorithm 2.
 - 6: Compute control input $u_i(k)$ for each MAP using (10).
 - 7: Update the position and velocity of each MAPs using the discretized MAP dynamics.
 - 8: **end while**
-

information about the key centers of network users. The connectivity potential function is defined as:

$$E_c^i(q) = k(\|q_1^r - q_i\|_\sigma + \|q_2^r - q_i\|_\sigma - \|q_1^r - q_2^r\|_\sigma). \quad (7)$$

where the σ -norm, $\|z\|_\sigma$ is defined as

$$\|z\|_\sigma = \frac{1}{\epsilon}(\sqrt{1 + \epsilon\|z\|^2} - 1), \quad (8)$$

with $\epsilon > 0$ a positive constant and the gradient can be expressed as

$$\nabla\|z\|_\sigma = \frac{z}{\sqrt{1 + \epsilon\|z\|^2}} = \frac{z}{1 + \epsilon\|z\|_\sigma}. \quad (9)$$

The advantage of $\|z\|_\sigma$ is that it is differentiable everywhere while traditional norm $\|z\|$ is not differentiable at $z = 0$. This creates a smooth potential function.

The effectiveness of the connectivity potential is shown in Fig. 3. Free MAPs can form a bridge between two clusters and provide connectivity.

C. MAP Dynamics

The control input u_i can be designed to consist of three components as follows [12]:

$$u_i = f_i(q, A, N_u) + g_i(p, A) + h_i(q, p), \quad (10)$$

where $f_i(q, A, N_u)$ defines the gradient based attractive and repulsive term, $g_i(p, A)$ defines the velocity consensus term and $h_i(q, p)$ defines the goal approach term.

- 1) Attractive and repulsive functions:

$$f_i(q, A, N_u) = \sum_{j \in N_i} \left[\Phi(\|q_j - q_i\|_\sigma) + a \left(1 - \alpha_{\{0,1\}} \left(\frac{\|(N_u^j - N^{max})^+\|_\sigma}{\|N^{max}\|_\sigma} \right) \right) \right] \mathbf{v}_{i,j}, \quad (11)$$

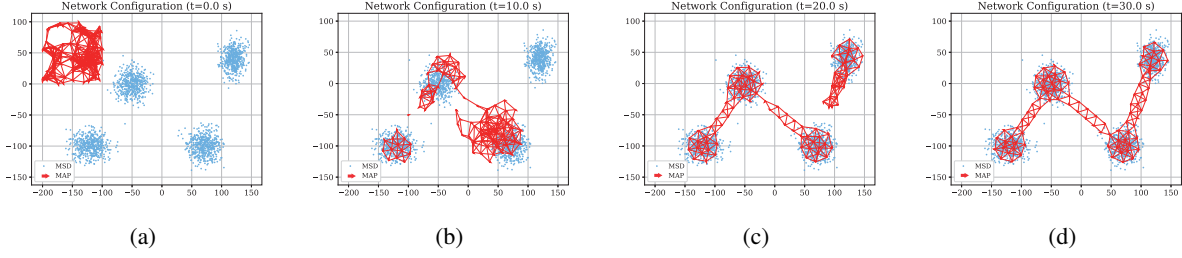


Fig. 2: Experiment results for network formation and connectivity. Figure (a) shows the initial positions of MAPs and MSDs. Figures (b), (c) and (d) show the process of MAPs covering all four MSD clusters and creating connectivity between them.

where $\mathbf{v}_{i,j} = \nabla \|q_j - q_i\|_\sigma$ is the vector from q_i to q_j . The function $\Phi(z)$ is expressed as:

$$\Phi(z) = \alpha_{\{0,1\}} \left(\frac{z}{\|r\|_\sigma} \right) \phi(z - \|d\|_\sigma), \quad (12)$$

where $\phi(z) = \frac{1}{2}[(a+b)\frac{(z+c)}{\sqrt{1+(z+c)^2}} + (a-b)]$ and $c = |a-b|/\sqrt{4ab}$ to ensure that $\phi(0) = 0$. Here r is the maximum communication range and d is the minimum distance between MAPs.

2) Velocity consensus function:

$$g_i(p, A) = \sum_{j \in N_i \setminus i} \left(1 - \alpha_{\{0,1\}} \left(\frac{\|(N^{max} - N_u^i)^+\|_\sigma}{\|N^{max}\|_\sigma} \right) \right) a_{ij}(p_j - p_i). \quad (13)$$

The velocity consensus function works as a damping force that leads to a match between neighboring MAPs. This can reduce potential collisions and disconnections between MAPs.

3) Goal functions:

We define a goal function based on the MAP mode $M_i(t)$. It shows a tendency to approach a dynamic/static group objective.

a) Goal function (for Mode M_0 and M_2):

$$h_i(q, p) = c_1(q_i^r - q_i) + c_2(p_i^r - p_i). \quad (14)$$

b) Goal function (for Mode M_1):

$$\begin{aligned} h_i(q, p) &= \nabla E_c(q) + \frac{1}{2}c_2(p_1^r - p_i) + \frac{1}{2}c_2(p_2^r - p_i) \\ &= \frac{k(q_1^r - q_i)}{1 + \epsilon \|q_1^r - q_i\|_\sigma} + \frac{k(q_2^r - q_i)}{1 + \epsilon \|q_2^r - q_i\|_\sigma} \\ &\quad + \frac{1}{2}c_2(p_1^r - p_i) + \frac{1}{2}c_2(p_2^r - p_i). \end{aligned} \quad (15)$$

D. Backhaul Connectivity Algorithm

We create a backhaul connectivity algorithm based on MAP modes $M_i(t)$. Suppose the centroids C_i of all MSD clusters are known. All MAPs are initialized

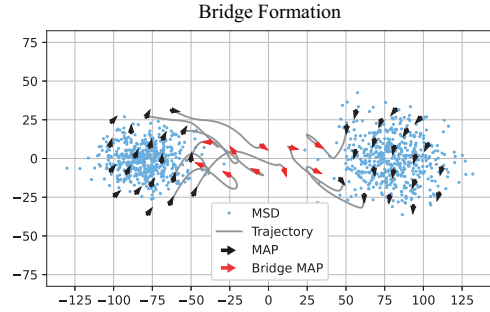


Fig. 3: An example of trajectories of MAPs connecting two clusters.

with random position $q_i(0)$, velocity $p_i(0)$ and mode $M_i(0) = M_0$. Then each MAP switches mode from $M_i(k)$ to $M_i(k+1)$ based on current mode $M_i(k)$, number of MSDs it serves $N_u^i(k)$ and the coverage ratio for current goal $r_g^i(k)$. When the MAPs switch to M_1 , they will establish connectivity between clusters using the connectivity functions defined in Equation 10. The detailed mode switch algorithms is defined in Algorithm 2.

V. SIMULATION RESULTS

In this section, we demonstrate the effectiveness of our proposed solution with simulations in Python platform. MAPs are released from a uniformly distributed area centered at $(-150, 50)$ with fixed height $h_i = 20$ m. The initial velocity of MAPs are randomly selected from $[-1, 1]^2$. The MSDs are divided into four clusters using 2D Gaussian distribution and each cluster has 500 MSDs for all simulations. The following parameters persist throughout the experiments: minimum separation between MAPs $d = 20$ m, communication range of MAPs $r = 1.2d$, $\epsilon = 0.1$ for $\|z\|_\sigma$, transmit power $\rho = 1$ W, path-loss exponent between MAPs and MSDs $\eta = 3.5$, $a = b = 5$ for $\phi(z)$, $N_{max} = 80$, $c_1 = 0.3$, $c_2 = 0.6$, $k = 10$ for goal functions, $r_0 =$

Algorithm 2 Mode Switch

Require: Current mode $M_i(k)$, Number of served MSDs $N_u^i(k)$, coverage ratio $r_g^i(k)$ for current goal $g_c^i(k)$, coverage thresholds r_0 , serving capacity thresholds n_0 and n_1 .

- 1: **if** $r_g^i(k) > r_0$ **then**
 - 2: Update MST of achieved goals $\mathcal{T}_c \leftarrow \mathcal{T}_c + g_c^i$.
 - 3: **if** $M_i(k) = M_0$ **then**
 - 4: **if** $0 < N_u^i(k) < n_0$ **then**
 - 5: Determine the nearest cluster center g_u^i that $g_u^i \notin \mathcal{T}_c$.
 - 6: Update current goal $g_c^i \leftarrow g_u^i$.
 - 7: **else if** $n_0 \leq N_u^i(k) < n_1$ **then**
 - 8: Update current mode $M_i(k) \leftarrow M_1$.
 - 9: Determine the clusters to connect using distributed MST algorithm [17] and build connectivity using the controller in Equation (10).
 - 10: **else**
 - 11: Update current mode $M_i(k) \leftarrow M_2$
 - 12: Serve MSDs in current goal cluster using the controller in (10) and (14)
 - 13: **end if**
 - 14: **else**
 - 15: $M_i(k) \leftarrow M_i(k)$
 - 16: **end if**
 - 17: **else**
 - 18: $M_i(k) \leftarrow M_i(k)$
 - 19: **end if**
-

0.95, $n_0 = 3$, $n_1 = 10$ for mode switching, Simulation time step $\Delta t = 0.1$ s.

In Fig. 2, we show an example of the experiment results for our proposed method using 90 MAPs. Fig. 2a shows the initialization of the MAPs and MSD. The MAPs traverse the four clusters, build connectivity between clusters and serve MSDs in their individual goal clusters. Finally at $t = 30.0$ s as shown in Fig. 2d, the network converge and develop a connected network covering all four clusters.

In Fig. 4 and Fig. 5, we compared the coverage ratios and Fiedler values using different number of MAPs. In situation when only 40 MAPs are deployed, the MAPs are unable to cover the fourth cluster due to the limitation of MAP quantity. The coverage ratio only reaches 70% after convergence. In situations when 40 or 60 MAPs are deployed, the Fiedler values remain zero after convergence because the network has insufficient MAPs to build connectivity among all clusters. In comparison, when 80 or 100 MAPs are deployed, the MAPs can form a desired connected network which cover all clusters with coverage ratios over 95%.

In Fig. 6, we analyze the resilience of the network

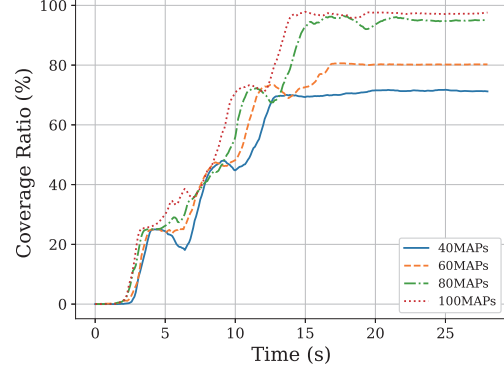


Fig. 4: Coverage ratios with time in experiments using different numbers of MAPs. The highest coverage ratio using 100 MAPs reaches 97.3% after convergence.

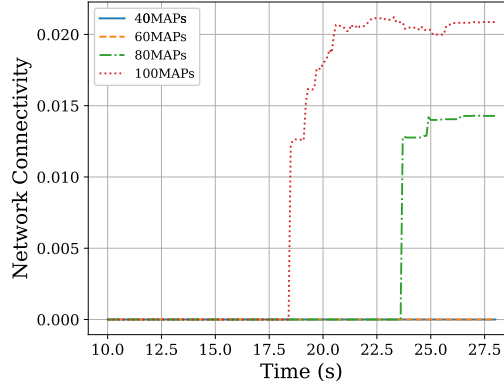


Fig. 5: Fiedler values with time in experiments using different numbers of MAPs. The highest Fiedler value using 100 MAPs reaches 0.021 after convergence.

when random failures of MAPs occur. 80 MAPs are used to build the network and random MAPs stop working at $t = 18$ s with failure ratios from 10.0% to 50.0%. With no failure happening, the coverage ratio keeps increasing until it reaches a highest value of 97%. When failure occurs at $t = 18$ s, the MAPs react quickly and restore coverage ratios. However, when the failure ratio is 50%, although the MAPs are still able to maintain a coverage ratio of 85%, the connectivity among clusters is lost.

In Fig. 7, we compare connectivity of the network (measured from Fiedler values after convergence) using different number of MAPs. When the number of MAPs is less than 65, the MAPs are unable to provide connectivity among all four clusters. So the Fiedler value in this case is zero. When the number of MAPs is between (65, 80), the Fiedler value increases drastically as the number of MAPs increases. When the number of MAPs is in the interval of (80, 120), the Fiedler value keeps increasing, however, the rate of increase reduces gradually.

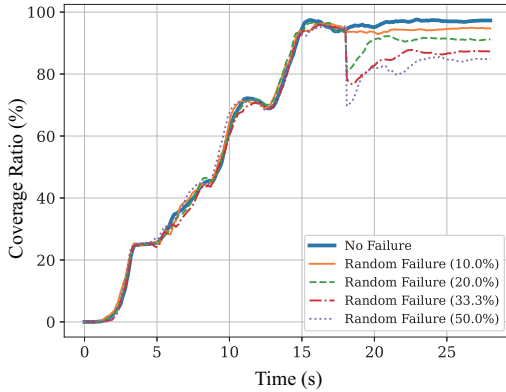


Fig. 6: Coverage ratios with time when random failure happens at $t = 18s$.

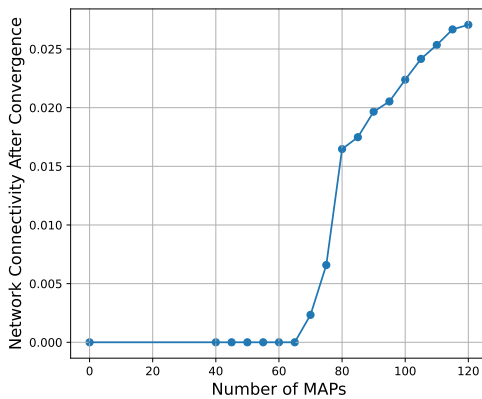


Fig. 7: Fiedler values after network convergence using different number of MAPs.

VI. CONCLUSIONS

In this paper, we presented a potential approach to construct a mobile aerial network that provides both local coverage and back-haul connectivity. The proposed method was inspired from flocking and distributed swarming behaviours in nature. The experimental results showed that the solution has been successful in maintaining a stable and high coverage ratio after the network converges. The designed connectivity algorithm was able to form communication bridges between spatially dispersed clusters. Further more, the network had resilience to random failures and self-recovery ability. Once failures occurred, the working UAVs can autonomously reconfigure the network and restore coverage and connectivity. In cases of extremely high failure ratios, the network may lose connectivity but can still provide local coverage around the cluster centers. Future work will focus on adding quality-of-service based coverage and connectivity to provide differentiated services in aerial networks.

REFERENCES

- [1] A. Fotouhi, H. Qiang, M. Ding, M. Hassan, L. G. Giordano, A. Garcia-Rodriguez, and J. Yuan, "Survey on UAV cellular communications: Practical aspects, standardization advancements, regulation, and security challenges," *IEEE Communications Surveys Tutorials*, vol. 21, no. 4, pp. 3417–3442, 2019.
- [2] M. Mozaffari, A. Taleb Zadeh Kasgari, W. Saad, M. Bennis, and M. Debbah, "Beyond 5G with UAVs: Foundations of a 3D wireless cellular network," *IEEE Transactions on Wireless Communications*, vol. 18, no. 1, pp. 357–372, 2019.
- [3] M. J. Farooq and Q. Zhu, "On the secure and reconfigurable multi-layer network design for critical information dissemination in the Internet of battlefield things (IoBT)," *IEEE Transactions on Wireless Communications*, vol. 17, no. 4, pp. 2618–2632, 2018.
- [4] T. Rains. (Sept. 2021) Take a look at AT&T's 'Flying COWs' - drones that returned cell service to hurricane Ida-hit Louisiana. [Online]. Available: <https://news.yahoo.com/look-ts-flying-cows-drones-113500471.html>
- [5] M. Jaber, M. A. Imran, R. Tafazolli, and A. Tukmanov, "5G backhaul challenges and emerging research directions: A survey," *IEEE Access*, vol. 4, pp. 1743–1766, 2016.
- [6] M. Melo, S. Nickel, and F. S. da Gama, "Facility location and supply chain management – A review," *European Journal of Operational Research*, vol. 196, no. 2, pp. 401–412, 2009.
- [7] M. Alzenad, A. El-Keyi, F. Lagum, and H. Yanikomeroglu, "3-D placement of an unmanned aerial vehicle base station (UAV-BS) for energy-efficient maximal coverage," *IEEE Wireless Communications Letters*, vol. 6, no. 4, pp. 434–437, 2017.
- [8] S. A. Al-Ahmed, M. Z. Shakir, and S. A. R. Zaidi, "Optimal 3D UAV base station placement by considering autonomous coverage hole detection, wireless backhaul and user demand," *Journal of Communications and Networks*, vol. 22, no. 6, pp. 467–475, 2020.
- [9] J. Cortes, S. Martinez, T. Karatas, and F. Bullo, "Coverage control for mobile sensing networks," *IEEE Transactions on Robotics and Automation*, vol. 20, no. 2, pp. 243–255, 2004.
- [10] M. Mozaffari, W. Saad, M. Bennis, and M. Debbah, "Efficient deployment of multiple unmanned aerial vehicles for optimal wireless coverage," *IEEE Communications Letters*, vol. 20, no. 8, pp. 1647–1650, 2016.
- [11] M. J. Farooq and Q. Zhu, "Cognitive connectivity resilience in multi-layer remotely deployed mobile Internet of things," in *IEEE Global Communications Conference (GLOBECOM 2017)*, 2017, pp. 1–6.
- [12] —, "A multi-layer feedback system approach to resilient connectivity of remotely deployed mobile Internet of things," *IEEE Transactions on Cognitive Communications and Networking*, vol. 4, no. 2, pp. 422–432, 2018.
- [13] R. Olfati-Saber, "Flocking for multi-agent dynamic systems: Algorithms and theory," *IEEE Transactions on Automatic Control*, vol. 51, no. 3, pp. 401–420, 2006.
- [14] R. Saber and R. Murray, "Flocking with obstacle avoidance: Cooperation with limited communication in mobile networks," in *42nd IEEE International Conference on Decision and Control (CDC 2003)*, vol. 2, 2003, pp. 2022–2028 Vol.2.
- [15] A. Al-Hourani and K. Gomez, "Modeling cellular-to-UAV path-loss for suburban environments," *IEEE Wireless Communications Letters*, vol. 7, no. 1, pp. 82–85, 2018.
- [16] M. A. Abdel-Malek, A. S. Ibrahim, and M. Mokhtar, "Optimum UAV positioning for better coverage-connectivity tradeoff," in *IEEE 28th Annual International Symposium on Personal, Indoor, and Mobile Radio Communications (PIMRC 2017)*, Montreal, QC, Canada, Oct. 2017.
- [17] R. G. Gallager, P. A. Humblet, and P. M. Spira, "A distributed algorithm for minimum-weight spanning trees," *ACM Transactions on Programming Languages and Systems (TOPLAS)*, vol. 5, no. 1, pp. 66–77, 1983.